An Accurate and Fast Computational Algorithm for the Two-diode Model of PV Module Based on Hybrid Method

Vun Jack Chin, *Student Member, IEEE*, Zainal Salam, *Member, IEEE* and Kashif Ishaque, *Member, IEEE*

***Abstract*—This paper proposes an improved hybrid method to compute the parameters of the two-diode model of photovoltaic (PV) module. Unlike previous methods, it attains the speed of the analytical approach by utilizing only datasheet information. Furthermore, its accuracy is not compromised as it does not require simplifications in its computation. Four parameters are determined analytically, while the remaining three are optimized by using an evolutionary algorithm, i.e. the differential evolution (DE). The speed is improved because the parameters are optimized only once, i.e. at standard test condition (STC), while the values at other conditions are computed analytically. Furthermore, a procedure to guide the initial conditions of the Newton-Raphson iteration is introduced. For validation, the algorithm is compared to other established computational methods for mono-, poly-crystalline and thin film modules. When evaluated against the experimental data, the mean absolute error is improved by one order of magnitude, while the speed is increased by approximately threefold. The standard deviation of the decision parameters over 100 independent runs is less than 0.1—which suggests that the optimization process is very consistent. Due to its speed and accuracy, the method is envisaged to be useful as a computational engine in PV simulator.**

***Index Terms*—differential evolution (DE), hybrid, parameter estimation, photovoltaic (PV), two-diode model.**

I. Introduction

FOR a successful realization of the solar PV system, the availability of an accurate, fast and reliable computer simulation tool is indispensable. The most crucial component that directly affects the accuracy of the simulator is the model of the cell (or module) itself. In PV literature, there are two equivalent circuit models, i.e. the single- and two-diode model [3]. These are lumped parametric models, in which the circuit equations define the current-voltage (*I*-*V*) relationships for any given irradiance (*G*) and temperature (*T*). The shape and amplitude of the *I*-*V* curve, in turn, are governed by the values of the model parameters, which have to be determined. Due to its intrinsic simplicity (i.e. fewer parameters), the single-diode model is more popular. However, recently, the two-diode version has gained attention owing to its superior accuracy [2, 4]. The improvement is primarily due to the inclusion of an extra diode, which represents the charge recombination process that is neglected in the single-diode model [3].

Notwithstanding this advantage, the two-diode model increases the complexities and consequently the computational burden. Now, the parameters to be determined is seven, compared to only five for the single-diode model. Due to the presence of two exponential terms and the implicit equations, obtaining the solution for these seven parameters is very challenging—which perhaps explains the limited reported works on the two-diode model. The parameters are normally solved in two ways: the numerical extraction or the analytical method. In the numerical extraction, a point-by-point fitting of the computed *I*-*V* values to the experimental dataset is carried out using certain mathematical algorithms. By defining an objective function, the model parameters are extracted by minimizing the error between the two [5-8]. Despite its accuracy, the approach inherits several drawbacks. First, to do the comparison, it is mandatory that the entire experimental *I*-*V* dataset is available. However, this information is not always given in the module datasheets [9]; hence, the application of the numerical extraction approach is highly situational. Second, due to the point-by-point comparison, the execution speed is very slow. This is especially true when evolutionary algorithm (EA), such as genetic algorithm, particle swarm optimization, etc., is utilized to optimize the curve fitting [5].

On the other hand, the analytical approach computes the model parameters by solving a system of equations, derived from several key points of the *I*-*V* curve. These points, namely the short circuit current (I_{SC}, 0), maximum power point (I_{MPP}, V_{MPP}), open circuit voltage (0, V_{OC}), temperature coefficients for short circuit current (K_i) and open circuit voltage (K_v), are commonly available in the standard datasheet [1, 2, 10]. Since

Manuscript received September 30, 2016; revised December 17, 2016 and January 25, 2017; accepted February 3, 2017. This work was supported by the Ministry of Science, Technology and Innovation (MOSTI), Malaysia, under Grant no. SF 03-01-06-SF1399.

Vun Jack Chin is with the Center of Electrical Energy Systems (CEES), Faculty of Electrical Engineering, Universiti Teknologi Malaysia, Johor Bahru, Malaysia (e-mail: vjchin2@live.utm.my).

Zainal Salam (corresponding author) is with the Center of Electrical Energy Systems (CEES), Faculty of Electrical Engineering, Universiti Teknologi Malaysia, Johor Bahru, Malaysia (e-mail: zainals@utm.my).

Kashif Ishaque is with the Department of Electrical Engineering, Mohammad Ali Jinnah University, Karachi, Pakistan (e-mail: kashif.ishaque@jinnah.edu).

there is no requirement to analyze the entire *I-V* curve, the number of iteration is much less, leading to much faster computation. Considering speed is an important factor for simulation, the analytical method is more practical. Despite this merit, the approach always involves certain simplifications on the two-diode model. This is inevitable due to the insufficient number of equations to independently determine the seven lumped parameters. Although these approximations simplify the computation, the solutions are compromised and at times, unrealistic. For example in [1], the saturation currents of both diodes are forced to assume equal magnitudes, i.e. $I_{o1} = I_{o2}$. This contradicts the fundamental concept, where I_{o2} is known to be few orders of magnitude greater than I_{o1} [11, 12]. Furthermore, the ideality factor of the second diode (a_2) is assigned to an arbitrary value which is greater than 1.2. The chosen value of a_2—whilst reduces the number of unknown parameters, cannot be physically justified. In another example, the authors in [2] disregarded the effects of both series (R_s) and shunt (R_p) resistances. By neglecting these resistances, the fitting accuracy of *I-V* curve is severely affected—particularly in the vicinity of V_{OC}. In another work [10], the ideality factors of the diodes are assumed to be related by $a_1 + a_2 = 3$ for polycrystalline and thin film, and $a_1 + a_2 = 4$ for amorphous cell. However, it is noted that these approximations do not work for all cell technologies [13]. More importantly, these relationships have no physical basis and are not always reliable [3, 14]. Apart from these works, other analytical methods are proposed in [12, 15, 16], but they tend to be tedious due to the introduction of many coefficients that complicate the computation. Quite often, the convergence is very poor, especially when incorrect initial conditions are selected [15, 17].

With the recent popularity of soft computing, a new approach—known as the hybrid method is proposed to compute the model parameters. As the name suggests, it incorporates both analytical and EA numerical extraction approaches. The analytical equations are employed to relate certain parameters to the variation of *G* and *T*, while the EA technique is used for optimization. Despite the improved accuracy [17-20], the hybrids are much slower because the EA processes have to be continuously executed throughout the simulation. In addition, they require additional information which are not available in the standard datasheet. For example, to use the scheme presented in [17, 18], the proprietary Sandia temperature coefficients are needed, while in [19, 20], the authors introduced new coefficients (α and β) to compute V_{OC} and V_{MPP}.

With regards to these shortcomings, this paper proposes a fast and accurate hybrid computational method for the two-diode model, which only requires standard datasheet information (i.e. V_{OC}, I_{SC}, V_{MPP}, I_{MPP}, K_i and K_v). The model parameters are computed in a two-phase process. First, I_{o2}, R_p, I_{o1} and I_{PV} are expressed analytically as functions of a_1, a_2, and R_s. With the correct values of a_1, a_2, and R_s, the exact corresponding values of I_{o2}, R_p, I_{o1} and I_{PV} can be directly computed. This effectively reduces the complexity of the model from seven to three unknown parameters. In the second phase, an EA, namely the differential evolution (DE) is used to search for the optimum and physically realizable values of a_1, a_2, and R_s. Using this approach, no approximations or omittance of certain parameters need to be made. Besides, unlike other hybrid solutions [17-20], the scheme retains the speed advantage of the analytical method. This is achieved by executing DE only once, i.e. prior to the simulation process. Thereafter, the well-established translational equations are employed to directly compute the model parameters with respect to the variations in *G* and *T*. By this way, the speed and inconsistency issues are eliminated. Another major contribution is the introduction of the guided initial condition procedures of the Newton-Raphson algorithm. It improves the computational speed by approximately three times compared to the popular analytical method suggested in [1].

In this work, DE is chosen for its remarkable ability in locating global optimum, fast convergence and low number of control parameters [13, 21]. Nonetheless, it is not mandatory to use DE—other EAs can be used too. To validate the proposed method, six modules of different technologies, i.e. mono-, poly-crystalline and thin-film are tested and benchmarked against well-established modelling methods for the two-diode model, namely the work by Ishaque *et. al* [1] and Babu and Gurjar [2].

II. The Two-diode PV Model

The two-diode model of a PV module is as shown in Fig. 1. Its output current is described by

$$I = I_{pv} - I_{o1}\left(e^{\frac{V+IR_s}{a_1V_t}} - 1\right) - I_{o2}\left(e^{\frac{V+IR_s}{a_2V_t}} - 1\right) - \frac{V+IR_s}{R_p} \tag{1}$$

where I_{PV} is the photocurrent, $V_t = N_s kT/q$ is the thermal voltage of the module with N_s cells connected in series, and I_{o1} and I_{o2} are the saturation current of the first and the second diode, respectively; a_1 and a_2 denote the ideality factors of the diodes; k is the Boltzmann constant (1.3806503×10^{-23} J/K); q is the electron charge (1.60217646×10^{-19} C); T is the temperature in Kelvin (K); R_s and R_p are the series and shunt resistance of the module, respectively. In total, the model requires the determination of seven unknown parameters, i.e. I_{PV}, I_{o1}, I_{o2}, a_1, a_2, R_s, and R_p. In addition to that, the values of these parameters vary with *G* and *T* as follows [22-24]:

$$a_i = a_{i,ref}, \quad i = 1, 2 \tag{2}$$

$$R_s = R_{s,ref} \tag{3}$$

$$R_p = R_{p,ref}\frac{G_{ref}}{G} \tag{4}$$

$$I_{o1} = I_{o1,ref}\left(\frac{T}{T_{ref}}\right)^3 e^{\frac{qE_g}{k}\left(\frac{1}{T_{ref}}-\frac{1}{T}\right)} \tag{5}$$

$$I_{o2} = I_{o2,ref}\left(\frac{T}{T_{ref}}\right)^{\frac{3}{2}} e^{\frac{qE_g}{a_2k}\left(\frac{1}{T_{ref}}-\frac{1}{T}\right)} \tag{6}$$

$$I_{SC} = \frac{G}{G_{ref}}\left[I_{SC,ref} + K_i(T - T_{ref})\right] \tag{7}$$

$$V_{OC} = V_{OC,ref} + K_v(T - T_{ref}) \tag{8}$$

where subscript "*ref*" denotes the reference parameters values at STC[1]; $E_g = E_{g,ref}[1\text{-}0.0002677\ (T - T_{ref})]$ is the material band gap energy expressed in eV ($E_{g,ref}$ = 1.121 eV for silicon, $E_{g,ref}$ = 1.04 eV for CIS thin film) [22]. Equations (2)-(8) are among the most established translational equations in the current PV literature [15, 22, 24-26]. Furthermore, they are simple to implement and do not require additional empirical information that are unavailable on the datasheet. These qualities make them ideal for the development of a generalized PV model. Nonetheless, the dependence of the model parameters on *G* and *T* remains an interesting and growing field of research [3, 27, 28]. In that regard, if an improved version of the translational equations is available in the future, they can be used in place of (2)-(8). The model parameters, when used in conjunction with the datasheet information, describes the electrical characteristics of the PV module. Therefore, the main objective of PV module modelling is to ensure that the *I-V* curves obtained by using the computed parameters closely matches the measured curves provided by the manufacturer.

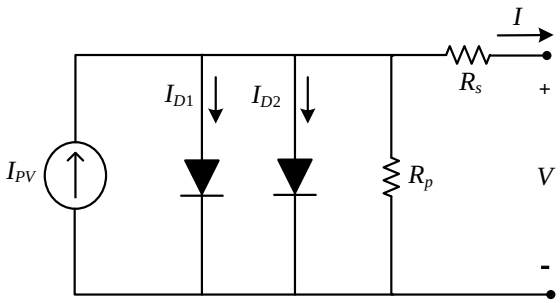

Fig. 1. The two-diode circuit model for the PV module.

III. Differential Evolution (DE)

DE is a stochastic real-valued parameter optimization technique [29, 30]. It is similar to genetic algorithm (GA); however, unlike GA—which relies mainly on the crossover, it employs mutation as the key mechanism to explore the search space. Like other members of the EA family, DE starts with a population of random candidate solutions, which is then refined through generations of mutation, crossover and selection operations. The processes are reiterated until the stopping condition fulfilled; that is a fitness value i.e. value-to-reach (*VTR*), or a maximum number of generations (Gen_{max}).

A. Initialization

DE begins by initializing a population of *NP D*-dimensional real-valued candidate solutions in the form of vectors: $X_{i,Gen} = [X_{1,i,Gen}, X_{2,i,Gen},.., X_{j,i,Gen},.., X_{D,i,Gen}]$; where *i* is the population index (i = 1, 2, …, *NP*), *D* denotes the number of decision variables (in this case, the model parameters), and *Gen* signifies the generation index. These vectors are randomly generated within a predefined search space, i.e.

$$X_{j,i,0} = X_L + rand[0,1](X_H - X_L) \tag{9}$$

where $X_L = [X_{1,L}, X_{2,L},…, X_{D,L}]$ and $X_H = [X_{1,H}, X_{2,H},…, X_{D,H}]$ are the lower and upper bound of the search space, respectively; while rand[0,1] is a random number generated between 0 and 1, following a uniform distribution. These vectors are also known as *target* vectors.

B. Mutation

For each target vector of the *Gen*-th generation, DE creates a *donor* vector, by summing the weighted difference between two random target vectors to a *base* vector, i.e.

$$V_{i,Gen} = X_{r1,Gen} + F(X_{r2,Gen} - X_{r3,Gen}) \tag{10}$$

where $r1$, $r2$ and $r3$ are distinct random integers ($r1 \neq r2 \neq r3 \neq i$). *F* is the mutation scaling factor, normally [0, 1].

C. Crossover

To diversify the population, a crossover operator is employed to create a population of *trial* vectors ($U_{j,i,Gen}$) by mixing the elements selected from $X_{j,i,Gen}$ and $V_{j,i,Gen}$. There are two types of crossover strategies, i.e. exponential and binomial crossover. In this work, the latter is chosen, i.e.

$$U_{j,i,Gen} = \begin{cases} V_{j,i,Gen}, & \text{if } (rand \le CR \text{ or } j = j_{rand}) \\ X_{j,i,Gen}, & \text{otherwise} \end{cases} \tag{11}$$

where $j_{rand} \in [1, 2…, D]$ is a random variable index, which guarantees $U_{i,Gen}$ acquires at least one element from $V_{i,Gen}$. However, the mutation process in conventional DE may cause the vectors to stray outside the predefined search boundaries, resulting in unfeasible solutions. To eliminate such occurrence, the following penalty function is employed [5]:

$$U_{i,Gen+1} = \begin{cases} U_{i,Gen+1} - rand[0,1](X_H - X_L), & \text{if } U_{i,Gen+1} > X_{iH} \\ U_{i,Gen+1} + rand[0,1](X_H - X_L), & \text{if } U_{i,Gen+1} < X_{iL} \end{cases} \tag{12}$$

D. Selection

To determine the population for the subsequent generation (*Gen* = *Gen* + 1), a tournament selection scheme is used, i.e.

$$X_{i,Gen} = \begin{cases} U_{i,Gen}, & \text{if } J(U_{i,Gen}) < J(X_{i,Gen}) \\ X_{i,Gen}, & \text{otherwise} \end{cases} \tag{13}$$

where $J(X)$ is the objective function to be optimized. If $U_{i,Gen}$ calculates a better fitness value than $X_{i,Gen}$, it will substitute $X_{i,Gen}$ in the population of the subsequent generation; otherwise, $X_{i,Gen}$ is retained. Thus, the overall fitness of the DE population will either improve or remain the same with each passing generation, but never deteriorates.

IV. The Proposed Hybrid Solution

The two-diode model requires the determination of seven model parameters, namely, I_{PV}, I_{o1}, I_{o2}, a_1, a_2, R_s, and R_p. To solve using the analytical method, a system of seven equations is needed. However, the standard module datasheet does not provide sufficient information to formulate these equations [1, 3]. Thus, numerous works are carried out to reduce the number of equations by making simplifications and approximations to the model [1, 2, 10]—which often results in a compromise to the accuracy of the solution. The alternative approach is the hybrid method [17-20]. However, it has several inherent disadvantages, as mentioned in the Introduction. In this work, an improved hybrid method is proposed to eliminate the speed, accuracy and inconsistency issues faced by the existing hybrid algorithms. The proposed solution is applicable to all types of modules as it requires only information found in the standard datasheet. Furthermore,

[1] STC: Standard test condition: G = 1000 W/m^2, T = 25 °C

to maintain the accuracy of the solution, the model parameters are computed without using any simplifications or approximations in their derivations.

A. Determination of the model parameters at STC

In the existing hybrid solutions, the EA is used to update the parameters values at every iteration during simulation. This process is lengthy and reduces the speed and consistency of the solution. In contrast, the proposed method only requires the parameters to be computed using EA once, i.e. at STC. Once the values of the parameters STC are known, a set of translational equations, i.e. (2)-(8), are employed to simulate the behavior of the module at other G and T conditions. The application of these equations ensure that the variations of the parameters are computed in accordance to the known physics of the solar cell.

Fundamentally, the proposed method can be described as a two-phase process. In the first phase, four parameters, i.e. $I_{o2,ref}$, $R_{p,ref}$, $I_{o1,ref}$ and $I_{PV,ref}$, are derived analytically as functions of $a_{1,ref}$, $a_{2,ref}$, and $R_{s,ref}$. To avoid cluttering of the equations, the following representations are used:

$$X_i = e^{\frac{I_{SC,ref} R_{s,ref}}{a_{i,ref} V_{t,ref}}}, \quad i = 1, 2 \tag{14}$$

$$Y_i = e^{\frac{V_{MPP,ref} + I_{MPP,ref} R_{s,ref}}{a_{i,ref} V_{t,ref}}}, \quad i = 1, 2 \tag{15}$$

$$Z_i = e^{\frac{V_{OC,ref}}{a_{i,ref} V_{t,ref}}}, \quad i = 1, 2 \tag{16}$$

In addition, the temperature dependence factors of the saturation currents, namely (5) and (6), are written as K_{o1} and K_{o2}, respectively. On the other hand, the shunt conductance, $G_{p,ref} = R_{p,ref}^{-1}$ is used in place of $R_{p,ref}$ for brevity. To obtain the first three equations, (1) is evaluated at three basic points of the I-V curve, i.e. the short circuit ($I = I_{SC}$, $V = 0$), open circuit ($I = 0$, $V = V_{OC}$), and maximum power point ($I = I_{MPP}$, $V = V_{MPP}$), i.e.

$$I_{SC,ref} = I_{PV,ref} - I_{o1,ref}(X_1 - 1) - I_{o2,ref}(X_2 - 1) - I_{SC,ref} R_{s,ref} G_{p,ref} \tag{17}$$

$$0 = I_{PV,ref} - I_{o1,ref}(Z_1 - 1) - I_{o2,ref}(Z_2 - 1) - V_{OC,ref} G_{p,ref} \tag{18}$$

$$I_{MPP,ref} = I_{PV,ref} - I_{o1,ref}(Y_1 - 1) - I_{o2,ref}(Y_2 - 1) - (V_{MPP,ref} + I_{MPP,ref} R_{s,ref}) G_{p,ref} \tag{19}$$

By algebraically manipulating (17)-(19), the expressions for $I_{PV,ref}$, $I_{o1,ref}$ and $G_{p,ref}$ can be written as (20)-(22), respectively.

$$I_{PV,ref} = I_{SC,ref} + I_{o1,ref}(X_1 - 1) + I_{o2,ref}(X_2 - 1) + I_{SC,ref} R_{s,ref} G_{p,ref} \tag{20}$$

$$I_{o1,ref} = \frac{I_{SC,ref} - I_{o2,ref}(Z_2 - X_2) - (V_{OC,ref} - I_{SC,ref} R_{s,ref}) G_{p,ref}}{Z_1 - X_1} \tag{21}$$

For the derivation of $I_{o2,ref}$, the fourth equation is obtained based on the idea that the model should always behave in accordance to the temperature coefficients specified by the manufacturer, i.e. K_i and K_v. Although similar concept is proposed for the single diode model [22], this information has never been utilized for the computation of the two-diode model parameters. Mathematically, it can be implemented by substituting (20) into (18), and evaluating the resultant equation at an arbitrary temperature T_x:

$$\begin{aligned} 0 = {} & I_{o1,ref} K_{o1} (Z_1' - X_1') + I_{o2,ref} K_{o2} (Z_2' - X_2') \\ & + \{V_{OC,ref} + K_v (T_x - T_{ref}) - [I_{SC,ref} + K_i (T_x - T_{ref})] R_{s,ref}\} G_{p,ref} \\ & - I_{SC,ref} - K_i (T_x - T_{ref}) \end{aligned} \tag{23}$$

where

$$X_i' = e^{\frac{[I_{SC,ref} + K_i (T_x - T_{ref})] R_{s,ref}}{a_{i,ref} V_{t,x}}}; \; Z_i' = e^{\frac{V_{OC,ref} + K_v (T_x - T_{ref})}{a_{i,ref} V_{t,x}}}, \quad i = 1, 2 \tag{24}$$

with $V_{t,x} = N_s k T_x / q$.

To ensure the computed parameter values remain relevant even at large temperature variations, the value of T_x should be chosen sufficiently far away from STC (in this work, T_x = 60 °C). Finally, by manipulating (20)-(23), $I_{o2,ref}$ can be expressed in its explicit form, given by (25). At this point, four analytical equations, i.e. (25), (22), (21) and (20) are established to facilitate the direct calculation of $I_{o2,ref}$, $R_{p,ref}$, $I_{o1,ref}$ and $I_{PV,ref}$, respectively. Since the only remaining unknowns are $a_{1,ref}$, $a_{2,ref}$, and $R_{s,ref}$, this effectively reduces the complexity of the model from seven unknown parameters to three. Thus, the challenge now is to define an appropriate objective function to determine these three parameters.

In the second phase of the algorithm, the values of $a_{1,ref}$, $a_{2,ref}$, and $R_{s,ref}$, are optimized using DE. These parameters serve as the ideal decision variables for optimization due to their small parametric ranges that allow for efficient exploration of the DE vectors. Since $a_{1,ref}$, $a_{2,ref}$, and $R_{s,ref}$ have pronounced effects at the knee of the I-V curve [14], their values can effectively be optimized by minimizing the gradient of the P-V curve at MPP. According to the basic power equation ($P = IV$), the derivative of power with respect to voltage can be written as:

$$\frac{dP}{dV} = V \frac{dI}{dV} + I \tag{27}$$

As dP/dV approaches zero at MPP, (27) becomes

$$0 = V_{MPP,ref} \left. \frac{dI}{dV} \right|_{at\ MPP} + I_{MPP,ref} \tag{28}$$

$$G_{p,ref} = \frac{I_{MPP,ref}(Z_1 - X_1) - I_{SC,ref}(Z_1 - Y_1) - I_{o2,ref}[(Z_2 - Y_2)(Z_1 - X_1) - (Z_1 - Y_1)(Z_2 - X_2)]}{(V_{OC,ref} - V_{MPP,ref} - I_{MPP,ref} R_{s,ref})(Z_1 - X_1) - (V_{OC,ref} - I_{SC,ref} R_{s,ref})(Z_1 - Y_1)} \tag{22}$$

$$I_{o2,ref} = \frac{I_{SC,ref} K_{o1} (Z_1' - X_1') + \{[I_{MPP,ref}(Z_1 - X_1) - I_{SC,ref}(Z_1 - Y_1)] W - [I_{SC,ref} + K_i (T_x - T_{ref})]\} (Z_1 - X_1)}{\{[(Z_2 - Y_2)(Z_1 - X_1) - (Z_2 - X_2)(Z_1 - Y_1)] W - K_{o2} (Z_2' - X_2')\} (Z_1 - X_1) + K_{o1} (Z_2 - X_2)(Z_1' - X_1')} \tag{25}$$

where

$$W = \frac{V_{OC,ref} + K_v (T_x - T_{ref}) - [I_{SC,ref} + K_i (T_x - T_{ref})] R_{s,ref} - \dfrac{K_{o1} (V_{OC,ref} - I_{SC,ref} R_{s,ref})(Z_1' - X_1')}{(Z_1 - X_1)}}{(V_{OC,ref} - V_{MPP,ref} - I_{MPP,ref} R_{s,ref})(Z_1 - X_1) - (V_{OC,ref} - I_{SC,ref} R_{s,ref})(Z_1 - Y_1)} \tag{26}$$

This article has been accepted for publication in a future issue of this journal, but has not been fully edited. Content may change prior to final publication. Citation information: DOI 10.1109/TIE.2017.2682023, IEEE Transactions on Industrial Electronics

Dividing both sides by $V_{MPP,ref}$ yields,

$$0 = \frac{dI}{dV}_{at\ MPP} + \frac{I_{MPP,ref}}{V_{MPP,ref}} \tag{29}$$

By using (29) as the objective function to be minimized, the fitness value, J, can be defined as,

$$J = \left| \frac{dI}{dV}_{at\ MPP} + \frac{I_{MPP,ref}}{V_{MPP,ref}} \right| \tag{30}$$

where

$$\frac{dI}{dV}_{at\ MPP} = \frac{-I_{o1,ref}\Gamma_1 Y_1 - I_{o2,ref}\Gamma_2 Y_2 - G_{p,ref}}{1 + I_{o1,ref}\Gamma_1 R_{s,ref} Y_1 + I_{o2,ref}\Gamma_2 R_{s,ref} Y_2 + G_{p,ref} R_{s,ref}} \tag{31}$$

$$\Gamma_1 = \frac{1}{a_{1,ref} V_{t,ref}};\ \Gamma_2 = \frac{1}{a_{2,ref} V_{t,ref}} \tag{32}$$

However, (21), (22) and (25) suggest that the incorrect combination of $a_{1,ref}$, $a_{2,ref}$, and $R_{s,ref}$ values may result in non-physical values of $I_{o1,ref}$, $R_{p,ref}$, and $I_{o2,ref}$. Hence, to ensure the algorithm always explore within the feasible region of the search space, the following penalty is imposed:

$$J = J_{rej} \text{ if } \begin{array}{l} R_p < R_{p,\min} \text{ or } R_p > R_{p,\max}; \text{ or} \\ I_{o1} < 0; \text{ or} \\ I_{o2} < 0; \text{ or} \\ I_{o2}/I_{o1} < 1 \end{array} \tag{33}$$

where $R_{p,min}$ and $R_{p,max}$ are the minimum and maximum values of $R_{p,ref}$, respectively. By this constraint, any vector that violates the limits specified in (33) is forced to assume an unusually large fitness value, J_{rej} (in this work, J_{rej} = 10). This prevents the vectors from being selected for the subsequent generation. Fig. 2 shows the overall flow of the proposed algorithm.

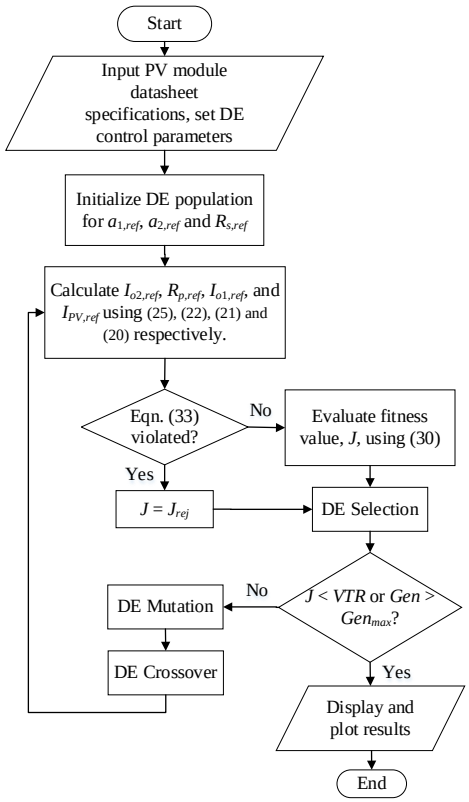

Fig. 2. Overall flow of the proposed algorithm.

B. Initial Values for the Newton-Raphson method (NRM)

Besides accuracy and consistency, computational speed is another aspect to be considered in the development of a practical simulator. Since the DE is executed only once, i.e. prior to the simulation process, the proposed method reduces the speed and inconsistency issues faced by the existing hybrid methods [17-20]. In addition to that, the speed is improved several times by guiding the initial values of output current during the Newton-Raphson (NRM) root-finding procedure. In its implicit form, (1), requires the continuous updating of I for every given value of V. The NRM progressively converges to the root $f(x)$ using the first-order polynomial of Taylor Series. At every iteration, a new approximation to the root is updated, i.e.

$$x^{iter+1} = x^{iter} - \frac{f(x^{iter})}{f'(x^{iter})} \tag{34}$$

In (34), superscript "*iter*" denotes the iteration number and $f'(x)$ is the derivative of a real-valued function $f(x)$. When applied to the two-diode model, the output current (I) for a given value of voltage can be calculated by solving

$$I_{ind}^{iter+1} = I_{ind}^{iter} - \frac{f(I_{ind}^{iter})}{f'(I_{ind}^{iter})} \tag{35}$$

where subscript "*ind*" denotes the element index of vector I. Furthermore,

$$f(I_{ind}^{iter}) = I_{PV} - I_{o1}\left(e^{\frac{V + I_{ind}^{iter} R_s}{a_1 V_t}} - 1\right) - I_{o2}\left(e^{\frac{V + I_{ind}^{iter} R_s}{a_2 V_t}} - 1\right) - \frac{V + I_{ind}^{iter} R_s}{R_p} - I_{ind}^{iter} \tag{36}$$

and

$$f'(I_{ind}^{iter}) = -\frac{I_{o1} R_s}{a_1 V_t} e^{\frac{V + I_{ind}^{iter} R_s}{a_1 V_t}} - \frac{I_{o2} R_s}{a_2 V_t} e^{\frac{V + I_{ind}^{iter} R_s}{a_2 V_t}} - \frac{R_s}{R_p} - 1 \tag{37}$$

Starting from an initial value of I, (35) is iteratively updated until $f(i)$ reaches a predefined error threshold, ε. In most works, it is customary to set the initial value of I to zero regardless of the corresponding value of V [31-33], i.e.

$$I_{ind}^{iter=0} = 0, \quad ind = 1, 2, 3 \ldots n \tag{38}$$

Although (38) does not impede the algorithm's ability to locate the root, it does however, imply that the initial value of I is far away from the final solution. This is because for most part of the I-V curve, the operating current of the PV module is much greater than zero. Consequently, the NRM routine is unnecessarily slow and thus, inefficient.

To improve the speed, a modification to the conventional NRM root-finding procedure is proposed. It is a priori from (17) that, when V = 0, $I = I_{SC}$, and depending on G and T, the value of I_{SC} can be determined by using (7). Therefore, for the first point of I (which starts at V = 0), a quick solution can be guaranteed by setting $I_{ind=1}^{iter=0} = I_{SC}$. On the other hand, the continuity of (1) dictates that the subsequent solution for I will always be in close proximity to the preceding solution. Therefore, it is reasonable to set $I_{ind}^{iter=0} = I_{ind-1}$ for the successive points (i.e. *ind* = 2, 3, 4… *n*). Fig. 3 shows the implementation of the improved NRM algorithm for computing the I-V characteristics. The proposed modification

This article has been accepted for publication in a future issue of this journal, but has not been fully edited. Content may change prior to final publication. Citation information: DOI 10.1109/TIE.2017.2682023, IEEE Transactions on Industrial Electronics

is drawn in dashed lines; it is executed in place of the greyed out sections of the NRM algorithm. Despite the simplicity of the modification, it is shown to reduce the computational time of the two-diode model by several times (refer to Section V).

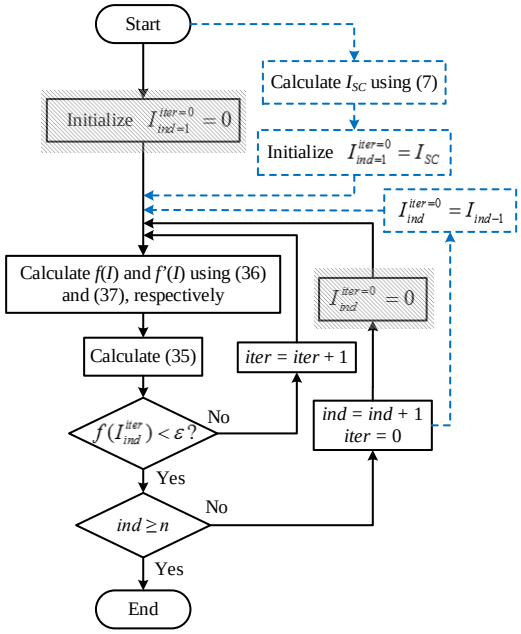

Fig. 3. Proposed improvement to the NRM algorithm for computing the *I*–*V* characteristics.

TABLE I
PV MODULES SPECIFICATIONS

Parameters	SP75	SM110-24	S25	RSM50	ST36	ST20
$I_{SC,ref}$ (A)	4.8	3.45	1.5	3.1	2.68	1.54
$V_{OC,ref}$ (V)	21.7	43.5	21.4	21.7	22.9	22.9
$I_{MPP,ref}$ (A)	4.4	3.14	1.45	2.82	2.28	1.28
$V_{MPP,ref}$ (V)	17	35	16.5	17	15.8	15.6
K_i (mA/°C)	2	1.4	0.7	1	0.32	0.2
K_v (mV/°C)	–76	–152	–76	–78	–100	–100
N_s	36	72	36	36	42	42

V. RESULTS AND DISCUSSION

For effective implementation, it is crucial to set the control parameters of DE correctly. Based on extensive trials, the optimal values of *F* and *CR* are chosen to be 0.5 and 0.8, respectively. There are no strict guidelines in selecting these values; in most cases, $F < 1$, while large value of *CR* promotes diversity in the population [21]. The DE strategy employed is DE/rand/1/bin. In this terminology, "rand" denotes random selection of base vector is employed in the mutation process, "1" signifies the number of difference vector, and "bin" represents the binomial crossover technique. Furthermore, for efficient optimization, the appropriate search ranges on the model parameters must be used. The value of a_1 is typically found in the vicinity between 1 and 2 [13]. Although a_2 is often assumed to be 2, but its actual value may vary up to 4 [11, 34]. On the other hand, modules have characteristically low value of R_s. Based on these information, the search boundaries of the model parameters are defined as follows: $a_1 \in [0.5, 2]$, $a_2 \in [2, 4]$, $R_s \in [0.01, 3]$.

The performance of the proposed computation method is validated by using six modules of different technologies, which include mono- and poly-crystalline as well as thin film. The experimental *I*-*V* data are extracted from the manufacturer's datasheet [35]. The specifications of the modules are summarized in Table I. Additionally, for better insight, the proposed method is compared against two popular published works, namely by [1] and [2].

A. Modelling Accuracy

Fig. 4 and 5 compare the accuracy the *I*-*V* characteristics for all three computational methods for varying *G* and *T*, respectively. Meanwhile, the STC parameters obtained are tabulated in Table II. For the mono- and poly-crystalline modules, the proposed model obtains a_1 and a_2 values close to 1 and 2 respectively. Furthermore, in contrast to [1], where both saturation currents are assumed to be equal, the optimized values for I_{o2} are found to be a few orders of magnitude larger than I_{o1}. These observations agree well with the fundamental theory of two-diode model [11, 12, 36]. Since the model parameters are highly correlated, i.e. the computation of one parameter greatly affects the rest, the simplifications used in [1] and [2] will inevitably introduce error in the computation of the remaining parameters.

For instance, as shown in Table II, the values of R_p computed by [1] are significantly lower than the proposed model for all modules. However, since the value of R_p accounts for the leakage current in p-n junction, its value is known to be relatively large in the actual modules (i.e. up to kΩ) [3]. Considering R_p greatly affects the shape of the curve in the region between the short circuit point and MPP [12], this explains why [1] tends to underestimate *I* at lower voltages, as observed in Fig. 4 and 5. In one specific case (for S25 module), method [1] obtains negative R_p—which is

TABLE II
COMPUTED MODEL PARAMETERS AT STC

Parameter	SP75			SM110-24			RSM50			S25			ST36			ST20		
	Prop.	Ishaque [1]	Babu [2]	Prop.	Ishaque [1]	Babu [2]	Prop.	Ishaque [1]	Babu [2]	Prop.	Ishaque [1]	Babu [2]	Prop.	Ishaque [1]	Babu [2]	Prop.	Ishaque [1]	Babu [2]
I_{PV}	4.803	4.800	4.800	3.453	3.450	3.450	3.102	3.100	3.100	1.500	1.500	1.500	2.684	2.680	2.680	1.549	1.540	1.540
I_{o1}	6.329E –10	3.106E –10	5.026E –05	4.249E –10	2.115E –10	1.335E –05	5.372E –10	2.006E –10	4.290E –05	2.542E –10	1.342E –10	1.872E –06	5.436E –07	1.628E –09	6.559E –03	4.819E –07	9.356E –10	6.351E –03
I_{o2}	1.052E –05	3.106E –10	1.302E –04	1.270E –05	2.115E –10	3.461E –05	8.791E –06	2.006E –10	1.112E –04	1.687E –06	1.342E –10	4.850E –06	8.402E –05	1.628E –09	1.699E –02	5.579E –05	9.356E –10	1.646E –02
a_1	1.042	1.000	2.046	1.044	1.000	1.887	1.061	1.000	2.097	1.031	1.000	1.702	1.665	1.000	3.528	1.753	1.000	3.862
a_2	2.059	1.300	4.394	2.118	1.300	3.621	2.027	1.300	4.681	2.147	1.300	2.960	2.062	1.300	88.827	2.094	1.300	168.950
R_s	0.394	0.445	0.000	0.707	0.926	0.000	0.551	0.688	0.000	0.779	1.584	0.000	1.254	1.862	0.000	2.378	3.463	0.000
R_p	633.932	126.210	∞	917.139	275.556	∞	1143.289	160.792	∞	2672.756	–408.928	∞	1044.676	96.758	∞	434.786	135.663	∞

This article has been accepted for publication in a future issue of this journal, but has not been fully edited. Content may change prior to final publication. Citation information: DOI 10.1109/TIE.2017.2682023, IEEE Transactions on Industrial Electronics

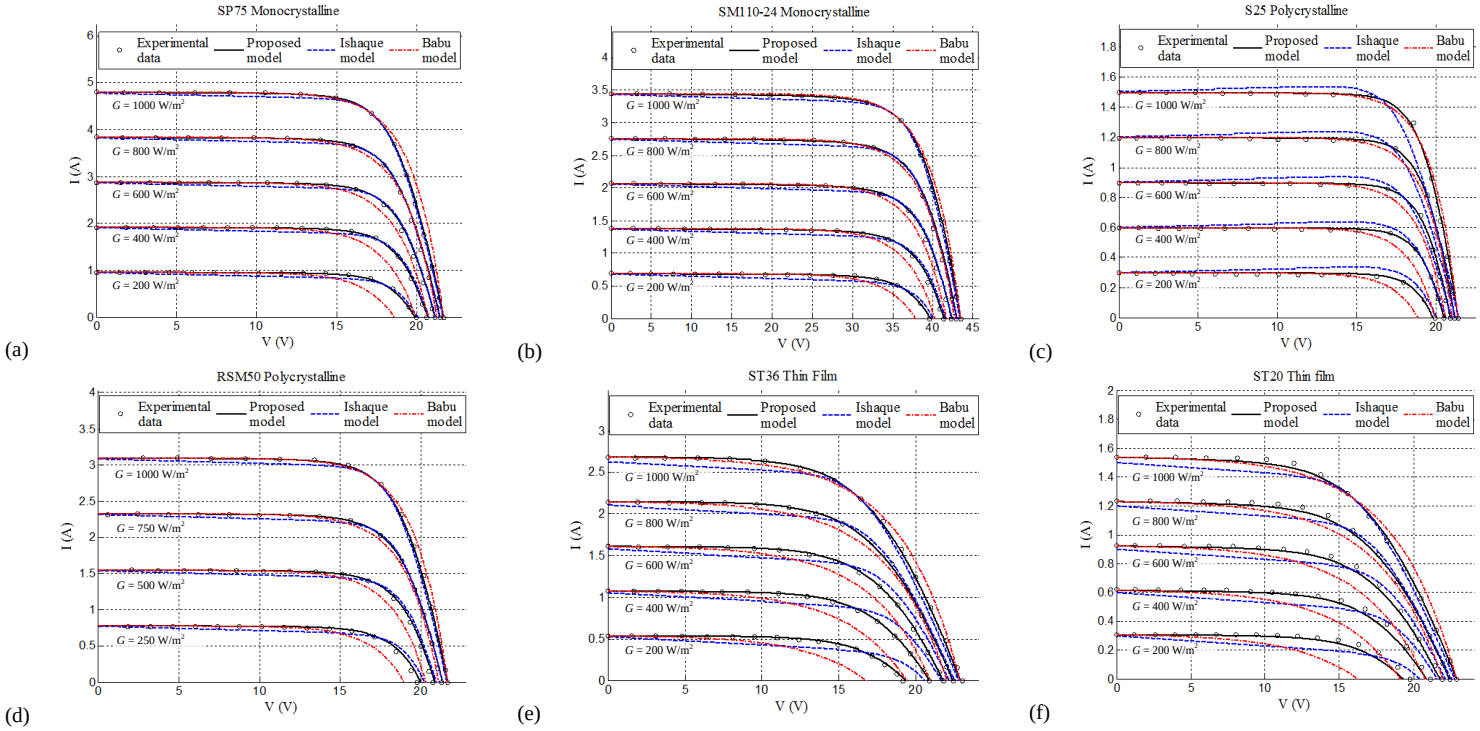

Fig. 4. *I–V* characteristics at varying irradiance (with T = 25°C) for a) SP75 b) SM110-24 c) S25 d) RSM50 e) ST36 f) ST20.

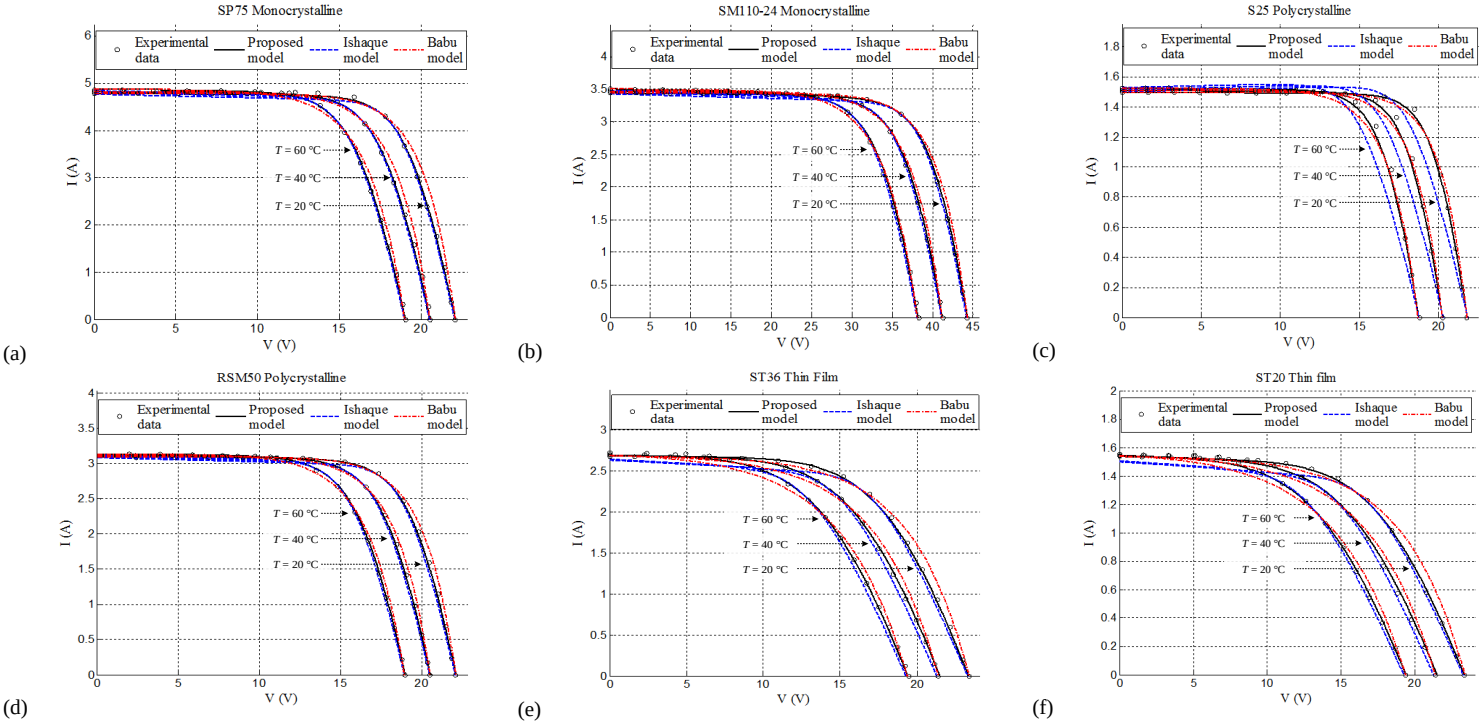

Fig. 5. *I–V* characteristics at varying temperature (with G = 1000 W/m^2) for a) SP75 b) SM110-24 c) S25 d) RSM50 e) ST36 f) ST20.

clearly an unacceptable value, regardless of how well the computed *I-V* curves fit the experimental data. More importantly, this implies that, despite the simplicity of the method proposed in [1], it does not always guarantee physically accurate results. On the other hand, the omittance of R_s and R_p in [2] indicates that the method is highly limited in its ability to accurately describe the output of the modules. Specifically, method in [2] consistently miscalculates the current output in the constant voltage region at low irradiance levels, regardless of the PV technology.

For the thin film modules (ST36 and ST20), the proposed model obtains relatively high value of R_s; this is consistent with the observations in [5, 13]. Moreover, the computed *I-V* curves closely matches the experimental data as shown in Fig. 4(e), 4(f), 5(e) and 5(f). In contrast, both [1] and [2] perform particularly poor for thin film modules. By assuming the same ideality factors (a_1 = 1, $a_2 \geq 1.2$) for all PV technologies,

This article has been accepted for publication in a future issue of this journal, but has not been fully edited. Content may change prior to final publication. Citation information: DOI 10.1109/TIE.2017.2682023, IEEE Transactions on Industrial Electronics

TABLE III
MEAN ABSOLUTE ERROR AT VARIOUS ENVIRONMENTAL CONDITIONS

Environmental conditions		SP75			SM110-24			RSM50*			S25			ST36			ST20		
G (W/m^2)	T (°C)	Prop.	Ishaque [1]	Babu [2]	Prop.	Ishaque [1]	Babu [2]	Prop.	Ishaque [1]	Babu [2]	Prop.	Ishaque [1]	Babu [2]	Prop.	Ishaque [1]	Babu [2]	Prop.	Ishaque [1]	Babu [2]
1000	25	0.022	0.038	0.145	0.025	0.035	0.070	0.018	0.068	0.054	0.014	0.060	0.032	0.017	0.081	0.061	0.014	0.047	0.044
800 (750)		0.035	0.053	0.074	0.028	0.044	0.035	0.017	0.038	0.049	0.010	0.041	0.021	0.010	0.056	0.064	0.013	0.044	0.055
600 (500)		0.029	0.063	0.155	0.021	0.052	0.075	0.023	0.063	0.096	0.010	0.029	0.047	0.009	0.092	0.142	0.017	0.052	0.102
400 (250)		0.015	0.060	0.201	0.015	0.054	0.101	0.021	0.056	0.081	0.006	0.0261	0.057	0.005	0.099	0.173	0.017	0.054	0.128
200		0.015	0.046	0.188	0.008	0.046	0.076	-	-	-	0.009	0.030	0.046	0.009	0.077	0.170	0.016	0.052	0.124
1000	20	0.029	0.075	0.13	0.018	0.048	0.061	0.022	0.063	0.062	0.009	0.065	0.024	0.022	0.081	0.062	0.008	0.041	0.042
	40	0.036	0.076	0.102	0.017	0.050	0.052	0.019	0.061	0.047	0.014	0.071	0.026	0.016	0.076	0.063	0.016	0.044	0.040
	60	0.034	0.064	0.102	0.029	0.051	0.053	0.008	0.051	0.045	0.016	0.080	0.027	0.024	0.081	0.061	0.012	0.040	0.043

method [1] results in a fixed curvature at the knee of the curve. Whilst such assumption describes the crystalline modules considerably well, it fails to account for the low fill factor inherent in the thin film. On the other hand, with the absence of module resistances, method [2] calculates unrealistically high values of a_1, a_2, I_{o1} and I_{o2}.

In addition, the disparities in term of I_{PV} values are observed to be particularly large for ST36 and ST20. This is because in contrast to the proposed method—where the exact value of I_{PV} is computed using (20), methods [1] and [2] assume $I_{PV} = I_{SC}$. Although the simplification is applicable for [2], it is bound to introduce certain degrees of error in [1] due to the residual voltage build-up in R_s at short circuit condition [37]. For cases such as ST36 and ST20, where the R_s to R_p ratios are relatively high, the error is more substantial. This is reflected in Fig. 4(e), 4(f), 5(e) and 5(f), where [1] visibly deviates from the experimental data in the short circuit current regions.

Table III summarizes the error of the modelling methods in term of mean absolute error (MAE). Note that, the corresponding values of G for RSM50 are written in brackets, as indicated by the asterisk. Among the three methods, the proposed model is observed to produce the lowest MAE. The difference in MAE is particularly substantial at low irradiances, where the MAE values of the proposed model is observed up to one order of magnitude lower than [2].

B. Simulation speed

Fig. 6 shows the convergence characteristics of the parameter optimization process using DE for 25 independent simulation runs. For a magnified view of the convergence characteristics, only $J \leq 0.1$ is shown in the figure. As an example, the Shell SM110-24 is used. The values of Gen_{max} and NP are set to 500 and 100, respectively. It can be observed that there are multiple instances where the population is initialized in unfeasible regions of the search space; these are indicated by the occurrences of high J values in the initial generations. Despite that, the algorithm manages to improve the solution and converges within a low number of iterations. On average, the algorithm converges to $J = 7.758\times10^{-6}$ in less than 300 generations, regardless of the initial values. The average elapsed time is 4.83 seconds when using the computer with Intel i5-2410M CPU 2.3 Ghz, 6 GB RAM.

Table IV compares the time required by each modelling method to compute the *I-V* curves in Fig. 4(b). Despite the fact that both the proposed method and [1] employ the standard two-diode model, the proposed model performs consistently faster in all cases (2.98 times faster on average). This is attributed to the modification to the NRM routine proposed in Section IV (B). By correctly guiding the initial value of I at the beginning of the iteration, the average number of NRM iteration required to compute each *I-V* curve is reduced significantly (2.4 times on average). The modification itself entails only minimal re-coding of the routine. On the other hand, the computation speed exhibited by [2] is the fastest. This is to be expected as the model has been reduced considerably by omitting R_s and R_p, at the expense of accuracy.

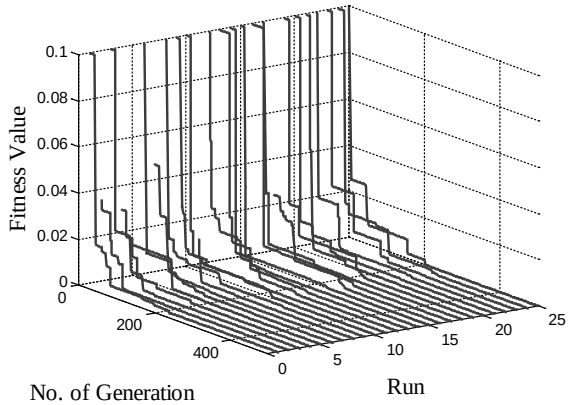

Fig. 6. Convergence characteristics of the parameter optimization process using DE for 25 independent runs.

TABLE IV
SIMULATION TIME

Environmental conditions		Proposed		Ishaque model [1]		Babu model [2]	
G (W/m^2)	T (°C)	Average NRM Iteration	Time (ms)	Average NRM Iteration	Time (ms)	Average NRM Iteration	Time (ms)
1000	25	1.852	3.494	4.455	10.145	-	0.986
800		1.833	3.377	4.413	10.025	-	0.996
600		1.813	3.324	4.339	9.901	-	1.006
400		1.794	3.290	4.323	9.897	-	0.998
200		1.774	3.231	4.273	9.857	-	1.009

C. Algorithm consistency

Like other members of the EA family, DE involves stochastic elements in its computation. Thus, it does not guarantee to yield the same solution at every single run. To investigate the consistency of the algorithm, statistical analyses are carried out. Since the rest of the model parameters are computed directly based on the values of $a_{1,ref}$, $a_{2,ref}$, and $R_{s,ref}$, they are not included in this discussion for brevity. Fig. 7 presents the solutions obtained for SP75 by

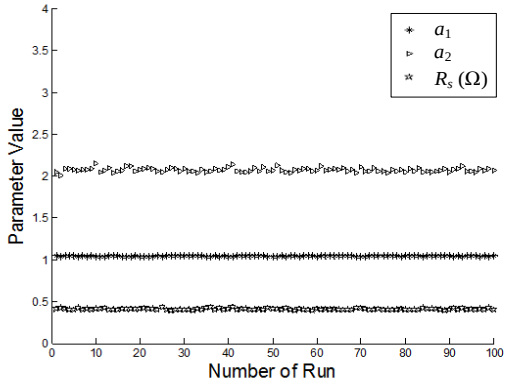

Fig. 7. DE decision parameters (a_1, a_2, and R_s) obtained over 100 runs for SP75.

executing the algorithm for 100 times. From the figure, a uniform pattern can be observed, i.e. the parameters always converge in a very concentrated region within the search space. This indicates that the proposed algorithm is highly successful in locating the global optimal/sub-optimal solution at each independent run. For a better insight, the mean and standard deviation (STD) for all six modules are computed, as shown in Table V. The STD values obtained are very low, i.e. less than 0.1 in all cases. The results suggest that a good quality solution is always guaranteed, i.e. high consistency—which is an important feature for a simulator.

The excellent performance of the algorithm can be attributed to several factors. First, the implementation of the penalty function in DE, i.e. (12), as well as the parameters constraints by (33) ensure that the exploration is within the physical ranges of the parameters. Second, the high values of *F* and *CR* enhance the diversity and exploration capability of the population. This helps prevent the vectors from getting trapped in the local optimal [30]. Third, the one-to-one selection scheme employed in DE instantaneously eliminates any vector that loses a single competition; therefore, only the best solutions are allowed to participate in the subsequent generation. Collectively, these factors contribute to highly accurate and consistent solutions.

TABLE V
MEAN AND STD OF DECISION PARAMETERS

Parameters		SP75	SM110-24	RSM50	S25	ST36	ST20
a_1	Mean	1.041	1.045	1.057	1.031	1.643	1.716
	STD	6.899E–04	0.002	0.001	0.002	0.080	0.062
a_2	Mean	2.071	2.086	2.075	2.156	2.062	2.142
	STD	0.024	0.028	0.031	0.046	0.015	0.042
R_s	Mean	0.405	0.690	0.589	0.779	1.258	2.325
	STD	0.009	0.029	0.018	0.013	0.010	0.039

VI. CONCLUSION

In this paper, an improved hybrid computational method for the two-diode model is presented. When evaluated against the experimental data of six different modules, the MAE of the proposed method is observed to be one order of magnitude lower than the other methods, especially at low irradiance conditions. This improvement is crucial for accurate prediction of the PV system performance as the irradiance level throughout the day is often much lower than STC. Furthermore, the accuracy at low irradiances is vital for reliable partial shading simulation. On the other hand, by introducing a simple procedure to guide the initial conditions of the NRM, the computational speed is improved by approximately threefold. In the simulation of large PV systems where numerous PV arrays are involved, this will contribute to significant reduction in computational time. With these merits, the proposed method is envisaged to be a valuable tool for the development of a reliable computational engine for a PV simulator.

ACKNOWLEDGMENT

The authors wish to acknowledge the Ministry of Science, Technology and Innovation Malaysia (MOSTI) for providing the financial assistance under the Science Fund Research Funding, SF 03–01–06–SF1399. The grant is managed by the Research Management Centre, Universiti Teknologi Malaysia, Skudai, Johor, Malaysia under vote number R.J130000.7909.4S119.

REFERENCES

[1] K. Ishaque, Z. Salam, and H. Taheri, "Simple, fast and accurate two-diode model for photovoltaic modules," *Solar Energy Materials and Solar Cells*, vol. 95, no. 2, pp. 586-594, 20/10, 2011.

[2] B. C. Babu, and S. Gurjar, "A Novel Simplified Two-Diode Model of Photovoltaic (PV) Module," *Photovoltaics, IEEE Journal of*, vol. 4, no. 4, pp. 1156-1161, 2014.

[3] V. J. Chin, Z. Salam, and K. Ishaque, "Cell modelling and model parameters estimation techniques for photovoltaic simulator application: A review," *Applied Energy*, vol. 154, no. 0, pp. 500-519, 9/15/, 2015.

[4] K. Ishaque, Z. Salam, and H. Taheri, "Accurate MATLAB simulink PV system simulator based on a two-diode model," *Journal of Power Electronics*, vol. 11, no. 2, pp. 179-187, 2011.

[5] K. Ishaque, Z. Salam, H. Taheri *et al.*, "A critical evaluation of EA computational methods for Photovoltaic cell parameter extraction based on two diode model," *Solar Energy*, vol. 85, no. 9, pp. 1768-1779, 2011.

[6] D. H. Muhsen, A. B. Ghazali, T. Khatib *et al.*, "Parameters extraction of double diode photovoltaic module's model based on hybrid evolutionary algorithm," *Energy Conversion and Management*, vol. 105, pp. 552-561, 11/15/, 2015.

[7] L. Sandrolini, M. Artioli, and U. Reggiani, "Numerical method for the extraction of photovoltaic module double-diode model parameters through cluster analysis," *Applied Energy*, vol. 87, no. 2, pp. 442-451, 9/8, 2010.

[8] L. Guo, Z. Meng, Y. Sun *et al.*, "Parameter identification and sensitivity analysis of solar cell models with cat swarm optimization algorithm," *Energy Conversion and Management*, vol. 108, pp. 520-528, 1/15/, 2016.

[9] S. A. Rahman, R. K. Varma, and T. Vanderheide, "Generalised model of a photovoltaic panel," *IET Renewable Power Generation*, vol. 8, no. 3, pp. 217-229, 2014.

[10] A. A. Elbaset, H. Ali, and M. Abd-El Sattar, "Novel seven-parameter model for photovoltaic modules," *Solar Energy Materials and Solar Cells*, vol. 130, pp. 442-455, 11//, 2014.

[11] M. Wolf, G. T. Noel, and R. J. Stirn, "Investigation of the double exponential in the current-voltage characteristics of solar silicon cells," *IEEE Transactions on Electron Devices*, vol. ED-24, no. 4, pp. 419-428, 1977.

[12] J. A. Gow, and C. D. Manning, "Development of a photovoltaic array model for use in power-electronics simulation studies," *Electric Power Applications, IEE Proceedings* -, vol. 146, no. 2, pp. 193-200, 1999.

[13] K. Ishaque, Z. Salam, S. Mekhilef *et al.*, "Parameter extraction of solar photovoltaic modules using penalty-based differential evolution," *Applied Energy*, vol. 99, no. 0, pp. 297-308, 11//, 2012.

[14] A. M. Humada, M. Hojabri, S. Mekhilef *et al.*, "Solar cell parameters extraction based on single and double-diode models: A review,"

Renewable and Sustainable Energy Reviews, vol. 56, pp. 494-509, 4//, 2016.
[15] M. Hejri, H. Mokhtari, M. R. Azizian *et al.*, "On the Parameter Extraction of a Five-Parameter Double-Diode Model of Photovoltaic Cells and Modules," *Photovoltaics, IEEE Journal of*, vol. 4, no. 3, pp. 915-923, 2014.
[16] S.-x. Lun, S. Wang, G.-h. Yang *et al.*, "A new explicit double-diode modeling method based on Lambert W-function for photovoltaic arrays," *Solar Energy*, vol. 116, pp. 69-82, 6//, 2015.
[17] K. Ishaque, and Z. Salam, "An improved modeling method to determine the model parameters of photovoltaic (PV) modules using differential evolution (DE)," *Solar Energy*, vol. 85, no. 9, pp. 2349-2359, 9//, 2011.
[18] V. J. Chin, Z. Salam, and K. Ishaque, "An accurate modelling of the two-diode model of PV module using a hybrid solution based on differential evolution," *Energy Conversion and Management*, vol. 124, pp. 42-50, 9/15/, 2016.
[19] N. Rajasekar, N. K. Kumar, and R. Venugopalan, "Bacterial Foraging Algorithm based solar PV parameter estimation," *Solar Energy*, vol. 97, pp. 255-265, 2013.
[20] B. Jacob, K. Balasubramanian, S. Babu T *et al.*, "Solar PV Modelling and Parameter Extraction Using Artificial Immune System," *Energy Procedia*, vol. 75, pp. 331-336, 8//, 2015.
[21] R. Storm, and K. Price, *Differential evolution—a simple and efficient adaptive scheme for global optimisation over continuous spaces*, ICSI Technical Report, 1995.
[22] W. De Soto, S. A. Klein, and W. A. Beckman, "Improvement and validation of a model for photovoltaic array performance," *Solar Energy*, vol. 80, no. 1, pp. 78-88, 1//, 2006.
[23] F. Attivissimo, A. Di Nisio, M. Savino *et al.*, "Uncertainty Analysis in Photovoltaic Cell Parameter Estimation," *Instrumentation and Measurement, IEEE Transactions on*, vol. 61, no. 5, pp. 1334-1342, 2012.
[24] F. Adamo, F. Attivissimo, A. Di Nisio *et al.*, "Characterization and Testing of a Tool for Photovoltaic Panel Modeling," *Instrumentation and Measurement, IEEE Transactions on*, vol. 60, no. 5, pp. 1613-1622, 2011.
[25] A. Laudani, G. Lozito, F. Mancilla-David *et al.*, "An improved method for SRC parameter estimation for the CEC PV module model," *Solar Energy*, vol. 120, pp. 525-535, 2015.
[26] A. Laudani, F. Mancilla-David, F. Riganti-Fulginei *et al.*, "Reduced-form of the photovoltaic five-parameter model for efficient computation of parameters," *Solar Energy*, vol. 97, no. 0, pp. 122-127, 11//, 2013.
[27] C. S. Ruschel, F. P. Gasparin, E. R. Costa *et al.*, "Assessment of PV modules shunt resistance dependence on solar irradiance," *Solar Energy*, vol. 133, pp. 35-43, 8//, 2016.
[28] N. Barth, R. Jovanovic, S. Ahzi *et al.*, "PV panel single and double diode models: Optimization of the parameters and temperature dependence," *Solar Energy Materials and Solar Cells*, vol. 148, pp. 87-98, 4//, 2016.
[29] S. Das, and P. N. Suganthan, "Differential Evolution: A Survey of the State-of-the-Art," *Evolutionary Computation, IEEE Transactions on*, vol. 15, no. 1, pp. 4-31, 2011.
[30] K. Price, R. M. Storn, and J. A. Lampinen, *Differential evolution: a practical approach to global optimization*: Springer, 2006.
[31] G. Walker, "Evaluating MPPT converter topologies using a MATLAB PV model," *Journal of Electrical & Electronics Engineering, Australia*, vol. 21, no. 1, pp. 49, 2001.
[32] S. Jing Jun, and L. Kay-Soon, "Photovoltaic Model Identification Using Particle Swarm Optimization With Inverse Barrier Constraint," *Power Electronics, IEEE Transactions on*, vol. 27, no. 9, pp. 3975-3983, 2012.
[33] M. G. Villalva, J. R. Gazoli, and E. R. Filho, "Comprehensive Approach to Modeling and Simulation of Photovoltaic Arrays," *Power Electronics, IEEE Transactions on*, vol. 24, no. 5, pp. 1198-1208, 2009.
[34] S. Chih-Tang, R. N. Noyce, and W. Shockley, "Carrier Generation and Recombination in P-N Junctions and P-N Junction Characteristics," *Proceedings of the IRE*, vol. 45, no. 9, pp. 1228-1243, 1957.
[35] "Shell PV Modules Datasheets," 2016; https://drive.google.com/open?id=0B1NbdRVXj_Gxb2JMTVRvT3lIVDg.
[36] D. S. H. Chan, and J. C. H. Phang, "Analytical methods for the extraction of solar-cell single- and double-diode model parameters from I-V characteristics," *Electron Devices, IEEE Transactions on*, vol. 34, no. 2, pp. 286-293, 1987.
[37] P. H. Huang, W. Xiao, J. C. H. Peng *et al.*, "Comprehensive Parameterization of Solar Cell: Improved Accuracy With Simulation Efficiency," *IEEE Transactions on Industrial Electronics*, vol. 63, no. 3, pp. 1549-1560, 2016.

Vun Jack Chin (IEEE Student Member) obtained his B.Eng (Hons) in Electrical Engineering from Universiti Tun Hussein Onn Malaysia (UTHM), Batu Pahat, Malaysia, in 2013. He is currently pursuing the Ph.D. degree (Electrical Engineering) at Universiti Teknologi Malaysia, Johor Bahru, Malaysia. His research interests include renewable energy, photovoltaic system modelling and control, soft computing, and power electronics.

Prof. Dr. Zainal Salam (IEEE Member) obtained his B.Sc (Electronics Engineering), M.E.E (Electrical Engineering). and Ph.D (Power Electronics), from the California State University (Chico, California), Universiti Teknologi Malaysia (UTM, Kuala Lumpur) and University of Birmingham (UK), in 1985, 1989 and 1997, respectively. He is currently the Professor in Power Electronics and Renewable Energy at the Centre of Electrical Energy Systems, Faculty of Electrical Engineering UTM. In 2011-2013 he was the Editor of IEEE Transaction on Sustainable Energy. He represents the country as the expert for the International Energy Agency (IEA) PV Power Systems Task 13 Working Group, which focus on the reliability and performance of PV power system. Prof. Zainal is the Vice-Chair of the IEEE Power Electronics, Industrial Electronics and Industry Application Joint Chapter, Malaysia Section (2011-2013, 2016). His main research interests include all areas of design, instrumentation and control of power electronics and renewable energy systems.

Dr. Kashif Ishaque (IEEE Member) received his B.E. from NED University, Pakistan, in 2006, Master of Engineering science and PhD from Universiti Teknologi Malaysia in 2009 and 2012, respectively. He is now an associate professor at Department of Electrical Engineering; Mohammad Ali Jinnah University (MAJU), Pakistan. He is also the Director of Office of Research Innovation and Commercialization (ORIC) at MAJU, which is responsible to promote and support the socio-economic research. Dr. Kashif is the author and co-author of nearly 50 publications in international journals and proceedings. His research interests include all areas of power electronics, renewable energy, intelligent control, and optimization algorithms for engineering applications.